Optimum Design and Performance of a Microwave Ladder Oscillator with Many Diode Mount Pairs

SHIGEJI NOGI AND KIYOSHI FUKUI, MEMBER, IEEE

Abstract—This paper presents a detailed discussion on the optimum design of a microwave ladder oscillator which is essentially an array of modules having a pair of diode mounts placed symmetrically with the waveguide-axis. A quantitative description of the power-combining mechanism for optimum operation is also given. The validity of the optimum design formula is confirmed by experiments on X-band oscillators with as many as twenty Gunn diodes, for which combining efficiency greater than 92 percent was obtained. Neither undesired single-mode nor simultaneous multimode oscillations were observed in the vicinity of the optimum circuit condition, and this was supported by mode-analytical discussion.

A ladder structure with equally spaced diode mount pairs is also treated because of its practical importance, and shown by theory and experiment to yield good combining efficiency.

I. Introduction

A NUMBER OF investigations have been carried out to combine output powers of many active devices, thereby achieving high-power microwave generation [1]. The multiple-device oscillator devised by Kurokawa and Magalhaes [2], [8] and the one by Harp and Stover [3] are among those known most prominently. The basic principle of these oscillators is that many devices are coupled with a common single cavity. They have, however, rather complicated structure in order to remove multimode difficulties.

Recently, the authors proposed a simpler multiple-device structure, consisting of an array of diode mount pairs in a rectangular waveguide [4]. As a prototype of this structure, a uniform line array of van der Pol oscillators mutually coupled by inductances and connected to a load (i.e., a multiple-device ladder oscillator) was treated using a mode-analysis approach to manifest its power-combining capability at the first mode and stable operation at the same mode [5]. While this mode analysis approach can successfully discuss the system behavior in broader aspects, it fails to describe the spatial variation of the voltage phase at each ladder section, and is almost impracticable for a nonuniform array structure. Thus, as a complementary approach, a general steady-state ac circuit analysis was carried out for a nonuniform microwave ladder structure, namely for the one with nonuniform spacing of successive mount pairs, to derive the optimum circuit condition for perfect power combining. The analytical results were confirmed by experiments for cases up to four mount pairs (eight diodes) [6]. The important thing is that, in a ladder structure with a few mount pairs, stable power-combining operation is found around the uniform spacing, while the theoretical condition for power combining itself is not restricted to the uniformly spaced case.

Last year, Y.-E. Ma and C. Sun developed a millimeter-wave eight Gunn diode combiner in a structure similar to the authors', and which showed a combining efficiency greater than 90 percent [7].

This paper describes the optimum design and performance of a microwave ladder oscillator with many more mount pairs, concentrating on the most practical structure of almost uniform spacing. A quantitative description of the power-combining mechanism and a physical interpretation of the optimum design are also given for better understanding. Section II recapitulates some basic matters in a microwave ladder oscillator necessary for the discussion in the following sections from [6]. In Section III, we derive the optimum design formula for the oscillator with an arbitrary number of diode mount pairs, and present equations for power flow distribution along the ladder structure which gives a better understanding of power-combining operation. Section IV is devoted to the discussion of power combining in a perfectly uniform array structure. In Section V, we give experimental results on the performance of microwave ladder oscillators with as many as ten diode mount pairs. Finally, in Section VI, stability of the desired mode operation is discussed using a highly approximate lumped-constant circuit model.

II. Structure of Oscillator and Basic Relations

The structure of a microwave ladder oscillator, shown in Fig. 1, is a series connection of waveguide sections each having a pair of diode mounts (we call this a mount pair for short in the following) placed symmetrically with the guide-axis. The resonant cavity is formed by the sliding short, the coupling window, and the sidewall of waveguide modified by the diode mount pair array. Assuming that the waveguide can propagate only in the dominant (TE_{10}) mode, two diode mounts forming a pair are in-phase oscillation which gives the equivalent representation shown in Fig. 2 for the kth diode mount pair. In this figure, the ith diode mount ($i=1,2$) of the kth mount pair is modeled by the parallel connection of the negative conductance

Manuscript received August 18, 1981; revised November 13, 1981.
The authors are with the Department of Electronics, Okayama University, 700 Okayama, Japan.

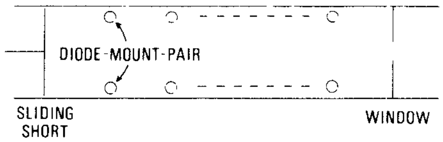

Fig. 1 Structure of a microwave ladder oscillator.

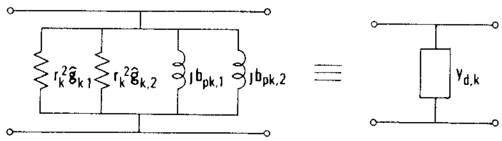

Fig. 2 Equivalent circuit of a diode mount pair

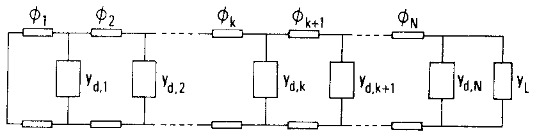

Fig 3. Equivalent circuit of a microwave ladder oscillator

$r_k^2\hat{g}_{k,i}$ and the inductive susceptance $b_{pk,i}$. The parameter $r_k(<1)$ represents the coefficient of coupling-reduction which arises because the diode mounts are displaced toward the sidewall of the waveguide: the terminal voltage of the diode mount is represented by $r_k v_k$, where v_k indicates the voltage at the guide-axis in the reference plane including the kth diode mount pair. Then, an equivalent circuit for a microwave ladder oscillator is given as shown in Fig. 3, where $y_L = g_L + jb_L$ denotes the normalized load admittance looking from the Nth diode mount pair[1], and ϕ_k is the electrical distance of the kth from the $(k-1)$th diode mount pair (from the shorting end for $k=1$). In the following analysis, we assume the voltage dependence of the negative differential conductance $\hat{g}_{k,i}$ as

$$\hat{g}_{k,i}(v_k) = -g_{0k,i} + 4r_k^2\theta_{k,i}v_k^2, \qquad k=1,2,\cdots,N, \quad i=1,2 \tag{1}$$

where $g_{0k,i} > 0$ and $\theta_{k,i} > 0$.

Assuming the steady state of angular oscillation frequency ω_0 and putting $v_k = V_k \exp\{j(\omega_0 t + \psi_k)\}$, we can derive the following relations for the fundamental harmonic components from the equations for the circuit in Fig. 3:

$$\sum_{l=1}^{k-1} (g_{l1} + g_{l2})V_l^2 = b_{tk}V_{k-1}V_k \sin\psi_{k,k-1} \tag{2}$$

$$\sum_{l=1}^{k-1} (-1)^{k-l} b_l V_l^2 = b_{tk}V_{k-1}V_k \cos\psi_{k,k-1}, \qquad k=2,3,\cdots,N \tag{3}$$

$$\sum_{k=1}^{N} (g_{k1} + g_{k2})V_k^2 + g_L V_N^2 = 0 \tag{4}$$

$$\sum_{k=1}^{N} (-1)^k b_k V_k^2 = 0 \tag{5}$$

[1]All admittances have been normalized by the characteristic admittance Y_0 of the waveguide

where $\psi_{k,k-1} = \psi_k - \psi_{k-1}$ and

$$g_{k1} + g_{k2} = -r_k^2(g_{0k,1} + g_{0k,2}) + r_k^4(\theta_{k,1} + \theta_{k,2})V_k^2, \qquad 1 \le k \le N \tag{6}$$

$$b_k = -\cot\phi_k + b_{pk,1} + b_{pk,2} - \cot\phi_{k+1}, \qquad 1 \le k \le N-1$$
$$b_N = -\cot\phi_k + b_{pN,1} + b_{pN,2} + b_L \tag{7}$$

$$b_{tk} = \csc\phi_k, \qquad 2 \le k \le N$$
$$b_{t1} = b_{t,N+1} = 0. \tag{8}$$

Equation (2) states that the sum of effective powers yielded by the diodes up to the $(k-1)$th diode mount pair flows through the line ϕ_k. Similary, (4) means that just the total power yielded by all the diodes is fed into the load. Equations (3) and (5) are the analogous relations concerning the reactive power. The $2N$ equations (2)–(5) can determine the values of $V_k(k=1,2,\cdots,N)$, $\psi_{k,k-1}(k=2,3,\cdots,N)$, and ω_0.

The maximum output power $P_{0,\max}$, the optimum voltage amplitude $V_{k,\text{opt}}$, and the optimum load conductance $g_{L,\text{opt}}$ can be derived from the requirement for maximizing the output power $P_0 = (1/2)g_L Y_0 V_N^2$. Using (4) and (6), these are given as

$$P_{0,\max} = \frac{Y_0}{8} \sum_{k=1}^{N} \frac{(g_{0k,1} + g_{0k,2})^2}{\theta_{k,1} + \theta_{k,2}} \tag{9}$$

$$V_{k,\text{opt}}^2 = \frac{g_{0k,1} + g_{0k,2}}{2r_k^2(\theta_{k,1} + \theta_{k,2})}, \qquad k=1,2,\cdots,N \tag{10}$$

and

$$g_{L,\text{opt}} = \frac{1}{2} r_N^2 (g_{0N,1} + g_{0N,2}) \sum_{k=1}^{N} \frac{\dfrac{(g_{0k,1} + g_{0k,2})^2}{\theta_{k,1} + \theta_{k,2}}}{\dfrac{(g_{0N,1} + g_{0N,2})^2}{\theta_{N,1} + \theta_{N,2}}} \tag{11}$$

respectively. Since the available power of each diode is equal to $Y_0 g_{0k,i}^2/(8\theta_{k,i})$ (9) states that the available powers of paired diodes add together perfectly as long as their parameters are equal to each other, and those of each mount pair can be combined perfectly. Note that the RF voltage amplitude at each diode mount $r_k V_k$ takes its inherent value independent of r_k in the power-combining condition, as indicated by (10).

III. Description of Optimum Operation

A. Optimum Design Formula

Consider the optimum circuit condition for maximizing the output power. In the following, we assume all the r_k, $g_{0k,i}$, $\theta_{k,i}$, and $b_{pk,i}$ values to be equal to each other, and put $r_k = r$, $g_{0k,1} + g_{0k,2} = g_0$, $\theta_{k,1} + \theta_{k,2} = \theta$, and $b_{pk,1} + b_{pk,2} = b_p$ $(k=1,2,\cdots,N)$, for simplicity. Then, (11) becomes

$$g_{L,\text{opt}} = \tfrac{1}{2}Nr^2 g_0 \tag{11'}$$

which shows that the optimum load conductance increases in proportion to the number of mount pairs. As all the $V_{k,\mathrm{opt}}$ values are equal to each other ($V_{k,\mathrm{opt}} = V_{\mathrm{opt}}$), which is seen from (10), (5) reduces to

$$\sum_{k=1}^{N} (-1)^k b_k = 0. \tag{12}$$

Elimination of $\psi_{k,k-1}$ from (2) and (3) leads to

$$\left\{\sum_{l=1}^{k-1} (-1)^l b_l\right\}^2 + \left(\frac{k-1}{2} r^2 g_0\right)^2 = b_{tk}^2, \qquad k = 2,3,\cdots,N. \tag{13}$$

When any two of ω_0, ϕ_1, $\phi_2, \cdots, \phi_N$, and b_L are given, the remainder can be determined using the N equations of (12) and (13).

We obtain from (12) and (7)

$$\begin{aligned} \cot\phi_1 + b_L &= 0, && \text{for even } N \\ -\cot\phi_1 + b_p + b_L &= 0, && \text{for odd } N. \end{aligned} \tag{14}$$

Similarly, we obtain from (13), (7), and (8)

$$-\cot\phi_1 + b_p - \cot\phi_k \pm \sqrt{\csc^2\phi_k - \left(\frac{k-1}{2} r^2 g_0\right)^2} = 0, \qquad \text{for even } k$$

$$\cot\phi_1 - \cot\phi_k \pm \sqrt{\csc^2\phi_k - \left(\frac{k-1}{2} r^2 g_0\right)^2} = 0, \qquad \text{for odd } k (k \geqslant 3) \tag{15}$$

which leads to

$$-\cot\phi_k = \frac{1}{2(-\cot\phi_1 + b_p)} \cdot \left\{1 - (-\cot\phi_1 + b_p)^2 - \left(\frac{k-1}{2} r^2 g_0\right)^2\right\}, \qquad \text{for even } k$$

$$-\cot\phi_k = \frac{1}{2\cot\phi_1} \cdot \left\{1 - (\cot\phi_1)^2 - \left(\frac{k-1}{2} r^2 g_0\right)^2\right\}, \quad \text{for odd } k (k \geqslant 3). \tag{16}$$

Equations (14) and (16) determine the optimum values of b_L and ϕ_k's ($k \geqslant 2$) for given values of ω_0 and ϕ_1. The phase differences between adjacent mount pairs are given from (2), (6), (8), and (10) as

$$\psi_{k,k-1} = -\sin^{-1}\left(\frac{k-1}{2} r^2 g_0 \sin\phi_k\right), \qquad k = 2,3,\cdots,N. \tag{17}$$

Equation (16) does not give a solution of equal $\phi_k (k \geqslant 2)$, so long as $r^2 g_0 \neq 0$; in other words, an exact equi-spacing structure cannot give perfect power combining. Thus, practically, we wish to seek an approximate equi-spacing structure with perfect power-combining capability. To meet this, we take as

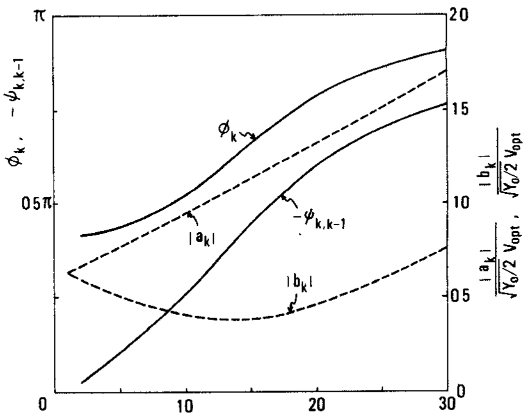

Fig. 4. Optimum designed electrical distance between the $(k-1)$th and the kth diode mount pair ϕ_k in the case of $b_p = -1.5$, $r^2 g_0 = 0.16$, and $\phi_1 = \cot^{-1}(b_p/2)$. Phase difference between two mount pairs, $\psi_{k,k-1}$, and normal variables $|a_k|$ and $|b_k|$ are also shown.

$$\phi_1 = \cot^{-1}\left(\frac{b_p}{2}\right) \equiv \phi_1^{(0)}. \tag{18}$$

This gives $b_L = -b_p/2$ regardless of N, and

$$-\cot\phi_k = \frac{1}{b_p}\left\{1 - \left(\frac{b_p}{2}\right)^2 - \left(\frac{k-1}{2} r^2 g_0\right)^2\right\}, \qquad \text{for any } k (\geqslant 2). \tag{16$'$}$$

$\phi_k (1 \leqslant k \leqslant N)$ is chosen to fall in the range $(0, \pi)$ since the fundamental mode operation is desirable from the viewpoint of stability. In the case of $b_p = -1.5$ and $r^2 g_0 = 0.16$, accordingly $\phi_1 = \phi_1^{(0)} = 0.705\ \pi$, the values obtained by (16)′ and (17) both for ϕ_k and $\psi_{k,k-1}$ are shown in Fig. 4. Denoting ϕ_k with $r^2 g_0$ neglected as

$$\phi^{(0)} \equiv -2\tan^{-1}\left(\frac{b_p}{2}\right) \tag{19}$$

we see from Fig. 4 that ϕ_k and $\psi_{k,k-1}$ take values close to $\phi^{(0)} = 0.410\ \pi$ and zero, respectively, for small k, and both of them increase up to π with increasing k. However, if we place the diode mount so close to the sidewall of waveguide that r and b_p are sufficiently small, all the ϕ_k's and $\psi_{k,k-1}$'s may remain very close to $\phi^{(0)}$ and zero, respectively, for a medium number of mount pairs.

The above statements can be better understood by using a Smith chart as follows. Let y_k and y_k' represent the admittances looking toward the load from the right and the left of the kth mount-pair, respectively, as shown in Fig. 5. As they are given by $y_k = jb_{d,k+1} + jb_{t,k+1} e^{j\psi_{k+1,k}} \cdot V_{k+1}/V_k$ and $y_k' = y_k + (-r^2 g_0/2 + jb_p)$, respectively, and using (2), (3), (6)–(8), and (10), we obtain

$$\left.\begin{matrix} y_k \\ y_{k+1}' \end{matrix}\right\} = \frac{k}{2} r^2 g_0 + (-1)^m \cdot j \cdot \left\{\begin{matrix} -\cot\phi_1, & \text{for even } k \\ \cot\phi_1 - b_p, & \text{for odd } k \end{matrix}\right\} \tag{20}$$

where we take $m = 0$ and $1 \leqslant k \leqslant N$ for y_k, and $m = 1$ and

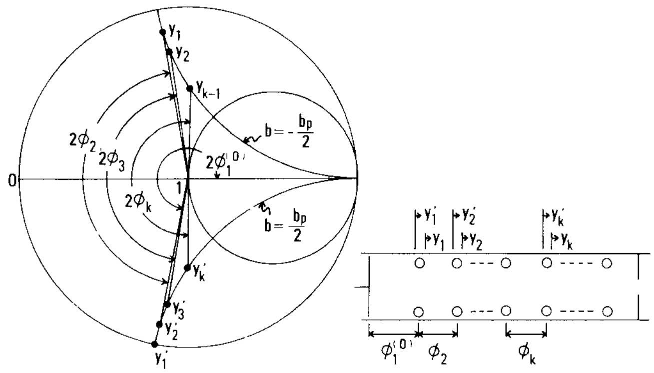

Fig 5 Admittances looking toward the load from each diode mount pair in the optimum condition plotted on a Smith chart.

$0 \leq k \leq N-1$ for y'_{k+1}. It can be seen from (20) that the conductance part of y_k is proportional to k while the susceptance part takes a constant value for each even and odd k. Under the condition of (18), the susceptance parts of y_k and y'_{k+1} take constant values $(-1)^m(-b_p/2)$ for all k. The Smith chart in Fig. 5 shows y_k's, y'_k's, and ϕ_k's in this case. From the figure, we can see that ϕ_k-values are close to $\phi^{(0)}$ for small k and increase up to π with increasing k.

B. Power Flow Distribution

Now we discuss the power flow distribution in a microwave ladder oscillator under the optimum condition. Consider a wave traveling toward the load and one traveling away from the load between $(k-1)$th and kth mount pairs, and denote these waves by the normal variables defined at the center of the line as a_k and b_k, respectively[2]. Then we have

$$\sqrt{\frac{Y_0}{2}}\, V_{\text{opt}} e^{j\psi_k} = a_k e^{-j\phi_k/2} + b_k e^{j\phi_k/2}, \qquad k=1,2,\cdots,N$$
$$= a_{k+1} e^{j\phi_{k+1}/2} + b_{k+1} e^{-j\phi_{k+1}/2}, \qquad k=1,2,\cdots,N-1. \tag{21}$$

By using (21), and the fact that the line ϕ_1 is shorted at its left end, we obtain (see Appendix I)

$$\left.\begin{matrix} a_1 \\ b_1 \end{matrix}\right\} = \pm\sqrt{\frac{Y_0}{2}}\, V_{\text{opt}} \cdot \frac{j}{2} \cdot \csc\phi_1 \cdot e^{j(\psi_1 \mp \phi_1/2)}$$
$$\left.\begin{matrix} a_k \\ b_k \end{matrix}\right\} = \sqrt{\frac{Y_0}{2}}\, V_{\text{opt}} \cdot \csc\phi_k \cdot \sin\frac{\phi_k \mp \psi_{k,k-1}}{2} \cdot e^{j(\psi_k+\psi_{k-1})/2},$$
$$k=2,3,\cdots,N. \tag{22}$$

This equation together with (16) and (17) gives

$$\left.\begin{matrix} |a_k|^2 \\ |b_k|^2 \end{matrix}\right\} = \frac{1}{8} Y_0 V_{\text{opt}}^2 \cdot \left[\left(\frac{k-1}{2} r^2 g_0 \pm 1\right)^2 + \left\{\begin{matrix} (-\cot\phi_1 + b_p)^2, & \text{for even } k \\ \cot^2\phi_1, & \text{for odd } k \end{matrix}\right\}\right], \qquad k=1,2,\cdots,N. \tag{23}$$

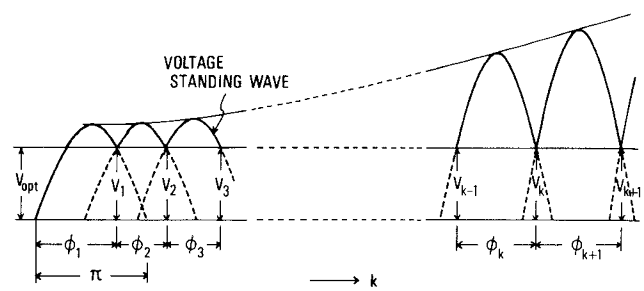

Fig 6. Voltage standing wave in a microwave ladder oscillator of optimum design.

In (22) and (23), the upper and the lower signs correspond to a_k and b_k, respectively. The power flow toward the load P_k through the line ϕ_k is given using (23) and (10) by

$$P_k = |a_k|^2 - |b_k|^2 = (k-1) \cdot \frac{Y_0}{8} \cdot \frac{g_0^2}{\theta}. \tag{24}$$

Equation (24) shows that P_k is equal to the sum of the available powers of the diodes up to the $(k-1)$th diode mount pair. Under the condition of (18), (23) results in the equation independent of odd or even k; a typical example of $|a_k|$ and $|b_k|$ is shown in Fig. 4. Refering to the reflection coefficient at the center of the line ϕ_k, $\Gamma_k = b_k/a_k$, we know from Fig. 4 that $|\Gamma_k|$ decreases from unity, reaches the minimum value at a certain value of k, and then increases up to unity again as k increases. $\Gamma_k (k \geq 2)$ is a real number as is apparent from (22), a fact which can also be understood from the Smith chart in Fig. 5. Accordingly, the voltage standing wave takes the maximum value of $\sqrt{2/Y_0}(|a_k| + |b_k|)$ at the center of the line ϕ_k, which increases with increasing k as seen in Fig. 4. These facts, together with the constancy of the voltage amplitude at each mount pair, lead to understanding that the optimum value of ϕ_k increases up to π with increasing k (Fig. 6).

IV. Power-Combining Capability of a Ladder Oscillator with a Uniform Diode Array

The results of the former section show that power combining in a microwave ladder oscillator with equally spaced mount pairs cannot be perfect. There is, however, much interest from the practical viewpoint in the power-combining efficiency of such an oscillator.

Equal spacing of mount pairs gives rise to deviations of b_k, b_{tk}, and V_k^2 from their optimum values $b_{k,\text{opt}}$, $b_{tk,\text{opt}}$, and $V_{k,\text{opt}}^2$, respectively. The deviations are denoted by Δb_k, Δb_{tk}, and $\delta_k V_{k,\text{opt}}^2$, respectively. Adjusting ϕ_1 and b_L to maximize the output power at the same oscillation frequency as the one in the optimum design, and denoting the deviations of $b_{d1} (\equiv -\cot\phi_1)$ and b_L from the optimum

[2] In this section, b_k is used as mentioned above. It indicates the susceptance defined by (7) elsewhere.

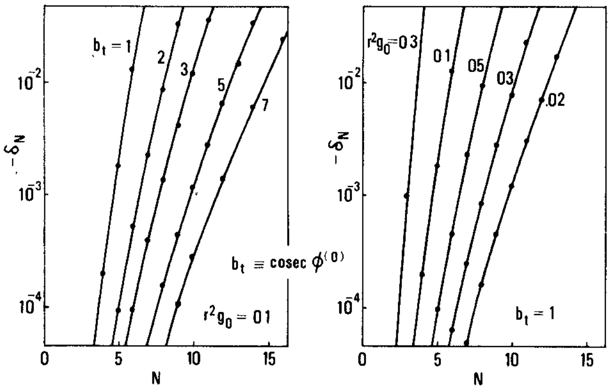

Fig. 7. Ratio of the output power drop to the perfectly combined power, $-\delta_N$, in a microwave ladder oscillator with equally spaced diode mount pairs.

ones as Δb_{d1} and Δb_L, respectively, we have

$$b_k = b_{k,\mathrm{opt}} + \Delta b_k + \Delta b_{d1}\delta_{k1} + \Delta b_L \delta_{kN}$$
$$V_k^2 = (1+\delta_k)V_{k,\mathrm{opt}}^2, \qquad k=1,2,\cdots,N \tag{25}$$

where δ_{kl} is the Kronecker delta. Substitution of (25) into (4) yields

$$\sum_{k=1}^{N} \delta_k^2 + N\delta_N = 0. \tag{26}$$

Substituting (25) into (5) and the equations obtained by eliminating $\psi_{k,k-1}$ from (2) and (3), and neglecting small terms of the second order, we get

$$\sum_{k=1}^{N} (-1)^k b_{k,\mathrm{opt}}\delta_k + (-1)^N \Delta b_L = \Delta b_{d1} - \sum_{k=1}^{N} (-1)^k \Delta b_k \tag{27}$$

and

$$\left\{\sum_{l=1}^{k-1} (-1)^{k-l} b_{l,\mathrm{opt}}\right\}\left\{\sum_{l=1}^{k-1} (-1)^{k-l} b_{l,\mathrm{opt}}\delta_l\right\} - \tfrac{1}{2} b_{tk,\mathrm{opt}}^2(\delta_{k-1}+\delta_k) = -\left\{\sum_{l=1}^{k-1} (-1)^{k-l} b_{l,\mathrm{opt}}\right\} \cdot\left\{(-1)^{k-1}\Delta b_{d1} + \sum_{l=1}^{k-1} (-1)^{k-1}\Delta b_l\right\} + b_{tk,\mathrm{opt}}\cdot \Delta b_{tk},$$
$$k=2,3,\cdots,N. \tag{28}$$

From (26)–(28), we can obtain the representations of δ_k and Δb_L with parameter Δb_{d1}. The ratio of the output power drop to the perfectly combined power is given by δ_N under the condition $d\delta_N/d\Delta b_{d1} = 0$. A calculated example of δ_N is shown in Fig. 7, for the case of $\phi_k = \phi^{(0)}$. As seen from Fig. 7, we have less drop in output power for larger $b_t (\equiv \csc\phi^{(0)})$ and for smaller r^2g_0. These can be achieved by placement of diode mounts closer to the sidewall of waveguide, because then b_p (accordingly $\phi^{(0)}$) diminishes.

V. Performance of Microwave Ladder Oscillators

Experiments were carried out using Gunn diodes GD511A manufactured by Nippon Electric Company. Fig. 8 shows the configuration of the X-band basic module with a diode mount pair. Each mount pair has characteristics a little different from each other. Table I shows the measured values for r^2g_0 and b_p and the maximum output powers in the case when each mount pair operates as a double-diode oscillator at 8.95 GHz[3]. Typical power-combining efficiency of a mount pair, that is, the ratio of the maximum output power of the double-diode oscillator with the mount pair to the sum of those of the two component diodes tested in optimized single-diode circuits, is 96 percent at 8.95 GHz. The frequency dependence of r^2g_0 and b_p is typically shown in Fig. 9. Both r^2g_0 and $|b_p|$ tend to decrease with frequency.

The oscillator with N mount pairs was constructed by using first N mount pairs in Table I in the following manner. We determined ϕ_1 for specified frequency by $\phi_1 = \cot^{-1}(\bar{b}_p/2)$ and $\phi_k (2 \leq k \leq N)$ by (16)′ with $b_p = \bar{b}_p$ and $r^2g_0 = \overline{r^2g_0}$, where the bar symbol as in $\bar{b}_p$ indicates the average value over N mount pairs. Spacing of mount pairs was adjusted using thin waveguide sections. The size and the position of the coupling window were determined so as to give the optimum load admittance: $g_{L,\mathrm{opt}} = (1/2)N\overline{r^2g_0}$ and $b_{L,\mathrm{opt}} = -\bar{b}_p/2$. A three-stub tuner, placed behind the coupling window, enabled fine adjustment of the load admittance. The microwave ladder oscillators constructed in this way were adjusted to maximize the output power at the given oscillation frequency by using the sliding short and the three-stub tuner. Table II shows the measured maximum output powers and the power-combining efficiencies of the oscillators with N mount pairs. The latter is taken as the ratio of the former to the sum of the maximum output power of the double-diode oscillators with each component mount pair. We can see from Table

[3]The r^2g_0-value is obtained using (11)′, that is, by doubling the measured value of the load conductance which maximizes the output power of the double-diode oscillator with the mount-pair.

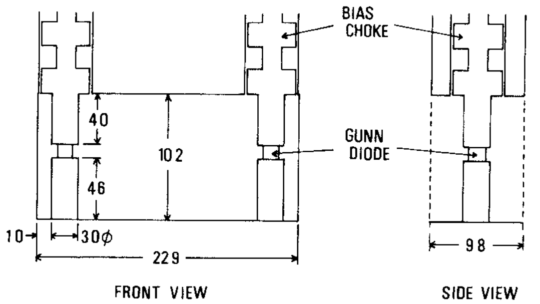

Fig. 8. Configuration of the X-band basic module with a diode mount pair. All dimensions are in millimeters.

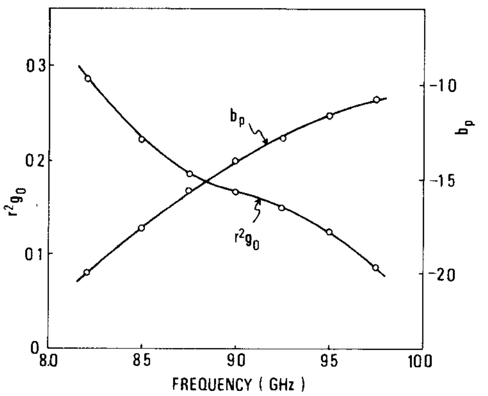

Fig. 9. Frequency dependence of $r^2 g_0$ and b_p of a diode mount pair.

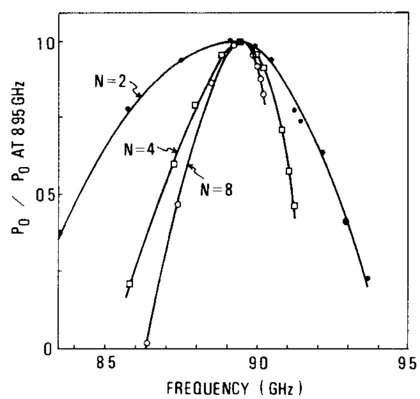

Fig. 10. Mechanical tuning characteristics of microwave ladder oscillators.

II that power-combining efficiency greater than 92 percent is attained for all the cases of $N \leq 10$. The deviation of the measured value of g_L and b_L from the calculated value from (11)′ and (14), respectively, were less than 15 percent for all N in Table II. The oscillation frequency can be varied by moving the sliding short in the vicinity of the optimum position (Fig. 11). The mechanical tuning characteristics thus obtained are shown in Fig. 10. The tuning range tends to decrease with increasing N.

Measurements were also carried out for the oscillator structure with equally spaced mount pairs mentioned in Section IV. For ϕ_k's, we used the value given by (19) with b_p replaced by $\bar{b}_p$. The values of g_L and b_L which maximize the output power were determined experimentally. Table III shows the measured results for $N \geq 6$. There were only negligible differences between the equi-spacing structure and the optimum design structure for $N \leq 4$. It can be seen from Tables II and III that the oscillator structure with equal spacing had power-combining efficiency only 0.6, 4.4, and 4.2 percent less than those of optimum design for $N = 6$, 8, and 10, respectively.

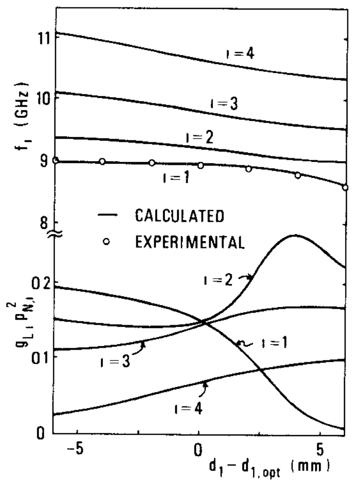

Fig. 11. Calculated values of the ith mode frequency f_i and $g_{L,i} p_{Ni}^2$ in (30) in the vicinity of the optimum condition, for the case $N = 6$. The measured values of oscillation frequency are also plotted for comparison.

TABLE I
CHARACTERISTICS OF DIODE MOUNT PAIRS ($f = 8.95$ GHz)

Mount-pair	$r^2 g_0$	b_p	Output power (mW)
No.1	0.157	-1.44	80.5
No.2	0.170	-1.43	72.2
No.3	0.188	-1.44	76.3
No.4	0.177	-1.44	76.3
No.5	0.176	-1.50	70.6
No.6	0.147	-1.54	62.6
No.7	0.171	-1.55	65.0
No.8	0.168	-1.62	64.9
No.9	0.157	-1.61	61.5
No.10	0.126	-1.52	57.5

TABLE II
RESULT OF POWER-COMBINING EXPERIMENTS UNDER OPTIMUM DESIGN ($f = 8.95$ GHz)

Number of mount-pairs	Number of diodes	Output power (mW)	Combining efficiency (%)
2	4	153	100.0
4	8	296	97.0
6	12	410	93.6
8	16	532	93.5
10	20	633	92.1

TABLE III
RESULT OF POWER-COMBINING EXPERIMENTS UNDER EQUAL SPACING DESIGN ($f = 8.95$ GHz)

Number of mount-pairs	Number of diodes	Output power (mW)	Combining efficiency (%)
6	12	408	93.0
8	16	506	89.1
10	20	604	87.9

VI. Stability of Desired-Mode Operation

In principle, there are an infinite number of normal oscillation modes in the resonant cavity of a microwave ladder oscillator. In this section, we consider the stability of each normal mode. A set of the voltage amplitudes at each mount pair for the ith mode is denoted as $\{p_{1i}, p_{2i}, \cdots, p_{Ni}\}$ in the unperturbed system obtained by removing all the conductances from the resonant cavity, where p_{ki}'s are assumed to satisfy

$$\sum_{k=1}^{N} p_{ki}^2 = 1. \tag{29}$$

Now, we define the following parameters as in [5]:

$$\alpha_i = r^2 g_0 - g_{L,i} p_{Ni}^2 \tag{30}$$

$$\theta_{ii} = r^4 \theta \sum_{k=1}^{N} p_{ki}^4$$

$$\theta_{ij} = 2r^4 \theta \sum_{k=1}^{N} p_{ki}^2 p_{kj}^2, \qquad i, j = 1, 2, \cdots, N \tag{31}$$

where $g_{L,i}$ represents the g_L-value at the ith mode frequency ω_i. α_i may be called a gain parameter for the ith mode, and θ_{ii} and θ_{ij} called self- and mutual-saturation parameters, respectively.

The stability condition for the oscillation at the ith mode is expressed as

$$\frac{\alpha_i}{\theta_{ii}} > \frac{\alpha_j}{\theta_{ji}}, \qquad \text{for all } j (\neq i), \qquad \text{with } \alpha_i > 0 \tag{32}$$

(see Appendix II). Equation (32) physically means that the presence of the ith mode with its steady-state amplitude makes the growth of the jth mode impossible. As for the possibility of simultaneous multimode oscillation, a necessary condition for stable oscillation of this type is that there is a mode-set (i, j) satisfying the inequalities

$$\frac{\alpha_i}{\theta_{ii}} < \frac{\alpha_j}{\theta_{ji}} \text{ and } \frac{\alpha_j}{\theta_{jj}} < \frac{\alpha_i}{\theta_{ij}}, \qquad \text{with } \alpha_i > 0, a_j > 0 \tag{33}$$

simultaneously (see Appendix II).

It is necessary for stable power-combining operation that neither undesired single-mode nor simultaneous multimode oscillations be stable. For the power-combining mode, that is, the first mode, we have

$$p_{k1}^2 = \frac{1}{N} \text{ and } g_{L,1} = \frac{1}{2} N r^2 g_0 \tag{34}$$

in the optimum design, and (30) and (31) become

$$\alpha_1 = (1/2) r^2 g_0$$
$$\theta_{11} = r^4 \theta / N$$
$$\theta_{1j} = \theta_{j1} = 2r^4 \theta / N. \tag{35}$$

Satisfaction of (32) by the mode is then obvious, and this guarantees the stability of the power-combining mode. It is not, however, an easy matter to examine analytically the stability of undesired modes and possible simultaneous multimodes, since finding analytical expression for p_{ki} is difficult.

For the microwave oscillators used in the experiment, it can be shown that only the power-combining mode is stable in the vicinity of the optimum design. Fig. 11 shows, for the case $N = 6$ as an example, the changes of the calculated values of $f_i (= \omega_i / 2\pi)$ and $g_{L,i} p_{Ni}^2$ with the change of the distance between the sliding short and the first mount pair d_1 around its optimum value $d_{1,\text{opt}}$ together with the measured values of oscillation frequency. Since $\alpha_i (i \neq 1)$ is negative in the vicinity of $d_1 = d_{1,\text{opt}}$ as seen from Fig. 11 and Fig. 9, neither (33) nor (32) can be satisfied for $i \neq 1$, which shows nonexistance of stable single and multimodes other than the desired mode. This agrees well with the experimental result. Measuring the oscillation frequency beyond the range of d_1 shown in Fig. 11, we found that the oscillation mode was unchanged for smaller d_1, while it turned into a double-mode of the first and the second modes near d_1 equal to a half wavelength for the second mode for $N \geqslant 4$. The appearance of the double-mode of these two modes can be explained as follows. According to the calculation based on the unperturbed system of the ladder oscillator, near the value of d_1 mentioned above, p_{1i} is the largest for $i = 1$ and approximately zero for $i = 2$. This results in small θ_{12}, and (33) obtains for these two modes. Thus, the double-mode comes about as a stable one, since α_1, $\alpha_2 > 0$ and $\alpha_l < 0$ for $l \geqslant 3$ as obtained using Fig. 9[4]. The method of discussing the mode stability in the above fails to be of good approximation for large N, because it uses the oscillation frequency and the voltage–amplitude distribution based on the unperturbed system. The deviation of the calculated result for the mode stability from the experimental one was shown to be nonnegligible, for $N \gtrsim 8$.

VII. Conclusion

We have given a detailed discussion on the optimum design for a microwave ladder oscillator with a large number of diode mount pairs. The validity of the optimum design formula has been confirmed by experiments for oscillators with as many as twenty Gunn diodes, for which combining efficiency greater than 92 percent was obtained. Stable power-combining operation in the experiments was ensured with the aid of mode-analytical discussion. A ladder oscillator with equi-spacing structure has also been treated and shown both by theory and experiment to exhibit good combining efficiency.

The oscillator described in this paper has a very simple structure, and accordingly has advantages in terms of easy manufacturability and small size. Another advantage is that an oscillator providing a certain required output power can be readily constructed simply by connecting an appropriate number of basic modules.

For an oscillator with many more mount pairs, some undesired modes might appear even in the vicinity of the power-combining condition, because then poorer mode separation results which brings more undesired modes into

[4]Though (33) represents only the necessary condition for the stable double-mode of the ith and the jth mode, (33) also becomes the sufficient one when a_l's $(l \neq i, j)$ are all negative.

the working frequency range of the active devices. In this case, it becomes necessary to use some conductances for suppressing the undesired modes as discussed in [5], and experimental investigation for this method will be needed for practical use. Diode mounts placed closer to the sidewall of the waveguide, which have smaller b_p, lead to smaller spacing of adjacent mount pairs in the optimum design. This separates the modes more from each other, and possibly enables only the first mode to be stable. Use of these mounts makes the equi-spacing structure more approximate to the optimum structure, which should serve to attain better combining efficiency. The power combiner of Kurokawa and Magalhaes [2], where $\phi_1 = \pi/2$ and $\phi_k = \pi$, can be considered to correspond to the case of $b_p = 0$.

Injection locking property of a microwave ladder oscillator[5] and application of the ladder structure to building a power-combining amplifier are other interesting subjects to be discussed; they are now being studied.

Appendix I

A. Derivation of the Representation for a_k and b_k

We get the ratio of voltages at each end of the line ϕ_k, v_k/v_{k-1}, and the ratio a_{k+1}/a_k from (21) as

$$\frac{v_k}{v_{k-1}} = e^{j(\psi_k - \psi_{k-1})} = \frac{a_k e^{-j\phi_k/2} + b_k e^{j\phi_k/2}}{a_k e^{j\phi_k/2} + b_k e^{-j\phi_k/2}}, \qquad k = 2,3,\cdots,N \quad (36)$$

and

$$\frac{a_{k+1}}{a_k} = \frac{e^{-j\phi_k/2} + \dfrac{b_k}{a_k} e^{j\phi_k/2}}{e^{j\phi_{k+1}/2} + \dfrac{b_{k+1}}{a_{k+1}} e^{-j\phi_{k+1}/2}}, \qquad k = 1,2,\cdots,N-1 \quad (37)$$

respectively. Equation (36) gives the reflection coefficient $\Gamma_k = b_k/a_k$ as

$$\frac{b_k}{a_k} = \frac{\sin\dfrac{\phi_k + \psi_{k,k-1}}{2}}{\sin\dfrac{\phi_k - \psi_{k,k-1}}{2}}, \qquad k = 2,3,\cdots,N. \quad (38)$$

As the line ϕ_1 is shorted at its left end, we have

$$a_1 = -b_1 e^{-j\phi_1}. \quad (39)$$

We can obtain (22) from (37)–(39) and the first equation of (21) for $k = 1$.

Appendix II

A. The Stability Condition of an Oscillation Mode in a Microwave Ladder Oscillator

For the purpose of discussing the stability of a oscillation mode, a microwave ladder oscillator may be appropriately modeled by a lumped-constant circuit system

[5]An experiment has shown that the locking bandwidth tends to increase with increasing N.

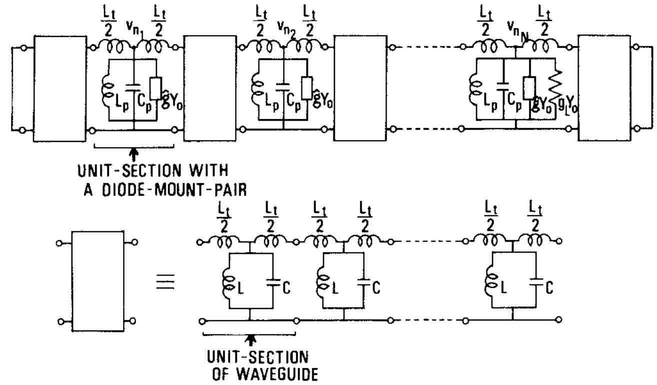

Fig. 12. Lumped-constant circuit model of a microwave ladder oscillator.

as shown in Fig. 12. The circuit is obtained by dividing the whole length of the resonant cavity (corrected by considering the effect of the coupling window) into $M(\gg N)$ sections. In Fig. 12, a unit-section of waveguide is represented by a equivalent circuit for TE_{10} waves, while each of N unit-sections including diode mount pairs is represented by a parallel connection of L_p and C_p in addition to $\hat{g}_{k,t}$ of (1). The values of L_p and C_p are determined by $b_p Y_0 = \omega C_p - 1/\omega L_p$ and the equation obtained by differentiation with respect to ω, with b_p and $\partial b_p/\partial\omega$ given in Fig. 9. Though the system of Fig. 12 has M normal modes, it is sufficient to consider only some lowest modes whose frequencies are included in the working range of the active devices.

We may write the circuit equations from Fig. 12 as

$$\frac{d^2 v_m}{d\tau^2} + \frac{1}{c_m}\left\{\frac{1}{l_m} + (2 + \delta_{m,1} + \delta_{m,M})\beta\right\} v_m - \frac{\beta}{c_m}\{(1+\delta_{m,1})v_{m-1} + (1+\delta_{m,M})v_{m+1}\}$$
$$= \frac{1}{\omega_c C_p}\left\{(r^2 g_0 - 4r^4\theta v_m^2)\delta_{m,n} - g_L \delta_{m,n_N}\right\}\frac{dv_m}{d\tau},$$
$$m = 1,2,\cdots,M;\ n = n_1, n_2, \cdots, n_N \quad (40)$$

where

$$\tau = \omega_c t \qquad \omega_c = \frac{1}{\sqrt{LC}} \qquad \beta = \frac{L}{L_t}$$

$$c_m = \frac{C_p}{C} \qquad l_m = \frac{L_p}{L}, \qquad \text{for } m = n_1, n_2, \cdots, n_N$$
$$c_m = 1 \qquad l_m = 1, \qquad \text{for } m \neq n_1, n_2, \cdots, n_N \quad (41)$$

and

$$v_0 = v_{M+1} = 0. \quad (42)$$

Therefore, the unperturbed system can be obtained by equating the right side of (40) to zero, i.e.,

$$\frac{d^2 \boldsymbol{v}}{d\tau^2} + \boldsymbol{B}\boldsymbol{v} = 0 \quad (43)$$

with

$$\boldsymbol{v} = [v_1, v_2, \cdots, v_M]^t \quad (44)$$

and the normal modes are represented by the eigenvectors of the matrix $\boldsymbol{B}$

$$\boldsymbol{p}_i' = [p_{1i}', p_{2i}', \cdots, p_{Mi}']^t, \qquad i=1,2,\cdots,M$$
$$\boldsymbol{p}_i'^t \boldsymbol{p}_j' = \delta_{ij}. \tag{45}$$

We also denote the eigenvalue corresponding to $\boldsymbol{p}_i'$ as λ_i.[6] Expanding $\boldsymbol{v}$ as

$$\boldsymbol{v} = \sum_{i=1}^{M} \boldsymbol{p}_i x_i \tag{46}$$

where x_i's are assumed to have the form

$$x_i = A_i \cos\left(\sqrt{\lambda_i}\,\tau + \psi_i\right) \tag{47}$$

we get the reduced differential equation from (40) such as[7]

$$\frac{dA_i^2}{d\tau} = \frac{1}{\omega_c C_p}\left(\alpha_i' - \theta_{ii}' A_i^2 - \sum_{j \neq i} \theta_{ij}' A_j^2\right) A_i^2 \tag{48}$$

where

$$\alpha_i' = r^2 g_0 \sum_{m=n_1,n_2,\cdots,n_N} p_{mi}'^2 - g_L p_{n_N,i}'^2$$
$$\theta_{ii}' = r^4 \theta \sum_{m=n_1,n_2,\cdots,n_N} p_{mi}'^4$$
$$\theta_{ij}' = 2r^4 \theta \sum_{m=n_1,n_2,\cdots,n_N} p_{mi}'^2 p_{mj}'^2 \qquad i,j=1,2,\cdots,M. \tag{49}$$

In the steady-state where only one mode, say the ith mode, is excited, the steady oscillation amplitude of this mode is given by (48) as

$$A_i^2 = \alpha_i' / \theta_{ii}' \tag{50}$$

where $\alpha_i' > 0$ and $\theta_{ii}' > 0$. The stability condition (the necessary and sufficient condition) for this mode is obtained from (48) as[7]

$$\alpha_i'/\theta_{ii}' > \alpha_j'/\theta_{ji}', \qquad \text{for all } j(\neq i). \tag{51}$$

The necessary condition for stable simultaneous multimode oscillation including the ith and the jth mode is given by (48) as[7]

$$\alpha_i'/\theta_{ii}' < \alpha_j'/\theta_{ji}'$$

and

$$\alpha_j'/\theta_{jj}' < \alpha_i'/\theta_{ij}'. \tag{52}$$

As the right side of (49) have the summation of p_{mi}' only at unit-sections with the active devices, it is convenient to use $p_{ki} = r_i p_{n_k i}'$ instead of p_{mi}', where r_i is determined so as to satisfy (29). Also define α_i, θ_{ii}, and θ_{ij} as (30) and (31) instead of α_i', θ_{ii}', and θ_{ij}', respectively. Then we obtain (32) and (33) instead of (51) and (52), respectively.

[6]Since $\boldsymbol{B}$ is not a symmetric matrix, its eigenvalues are not necessarily real number. But, physically, it is quite certain that all the eigenvalues are real and the corresponding eigenvectors have their elements of real number.

[7]See [5] to know the method of deriving (48), (51), and (52).

Acknowledgment

The authors wish to thank S. Tanaka and H. Murakami for their considerable assistance in the course of experiments.

References

[1] K. J. Russell, "Microwave power combining techniques," *IEEE Trans. Microwave Theory Tech.*, vol. MTT-27, pp. 472–478, May 1979.

[2] K. Kurokawa, and F. M. Magalhaes, "An *X*-band 10-W multiple-diode oscillator," in *Proc. IEEE*, vol. 59, pp. 102–103, Jan. 1971.

[3] R. S. Harp and H. C. Stover, "Power combining of *X*-band IMPATT circuit modules," presented at *IEEE Int. Solid-State Circuits Conf.*, Feb. 1973.

[4] K. Fukui and S. Nogi, "A multiple-diode structure for high-power Microwave generation," *IEEE MTT Int. Microwave Symp. Digest*, pp. 357–359, June 1978.

[5] K. Fukui and S. Nogi, "Power combining ladder network with many active devices," *IEEE Trans. Microwave Theory Tech.*, vol. MTT-28, pp. 1059–1067, Oct. 1980.

[6] K. Fukui and S. Nogi, "A microwave multiple-diode ladder oscillator," *Trans. IECE Japan*, vol. J64-B, pp. 816–823, Aug. 1981.

[7] T. -E. Ma and C. Sun, "1-W millimeter-wave Gunn diode combiner," *IEEE Trans. Microwave Theory Tech.*, vol. MTT-28, pp. 1460–1463, Dec. 1980.

[8] K. Kurokawa, "The single-cavity multiple-device oscillator," *IEEE Trans. Microwave Theory Tech.*, vol. MTT-19, pp. 793–801, Oct. 1971.

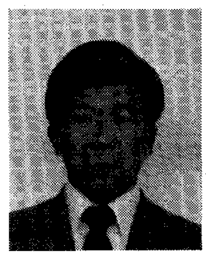

Shigeji Nogi was born in Osaka Prefecture, Japan, on December 26, 1945. He received the B.E. and M.E. degrees in electronics engineering from Kyoto University, Kyoto, Japan, in 1968 and 1970, respectively.

From 1970 to 1972 he was employed by the Central Research Laboratory, Mitsubishi Electric Corporation, Amagasaki, Japan. In 1972 he joined the Department of Electronics, Okayama University, where he has been engaged in research on microwave active circuits, multimode oscillators, and nonlinear wave propagation.

Mr. Nogi is a member of the Institute of Electronics and Communication Engineers of Japan.

Kiyoshi Fukui (M'75) was born in Tokushima Prefecture, Japan, on January 13, 1930. He received the B.Sc. degree in physics in 1952 and the D.Eng. degree in electronics engineering in 1964, both from Kyoto University, Kyoto, Japan.

From 1958 to 1962 he was a Research Assistant at the Department of Electronics, Kyoto University. From 1962 to 1967 he taught as an Assistant Professor at the Training Institute for Engineering Teachers, Kyoto University. In 1967 he became a Professor of Electronics at the Himeji Institute of Technology, Himeji, Japan. Since 1971 he has been with the Department of Electronics, Okayama University. His research interest has been mainly in nonlinear phenomena in electronics such as locking phenomena in oscillators, frequency multiplication by variable capacitance, behavior of multiple-device structures, and nonlinear wave propagation.

Dr. Fukui is a member of the Institute of Electronics and Communication Engineers of Japan and the Physical Society of Japan.